Global J. Environ. Sci. Manage. 6(3): 289-308, Summer 2020

Global Journal of Environmental Science and Management
(GJESM)

Homepage: https://www.gjesm.net/

ORIGINAL RESEARCH PAPER

Hydrodynamics and water quality assessment of a coastal lagoon using environmental fluid dynamics code explorer modeling system

F.M. Torres-Bejarano[1,*], A.C. Torregroza-Espinosa[2], E. Martínez-Mera[3], D. Castañeda-Valbuena[4], M.P. Tejera-González[5]

[1]*Departamento de Ingeniería Ambiental, Universidad de Córdoba, Carrera 6 No. 77- 305, Montería, Colombia*

[2]*Departamento de Gestión Industrial, Agroindustrial y de Operaciones, Universidad de la Costa, Barranquilla, Colombia*

[3]*Doctorado en Ciencias Biológico-Agropecuarias, Universidad Autónoma de Nayarit, México*

[4]*Instituto Tecnológico de Tuxtla Gutiérrez, Depto. Ingeniería Química y Bioquímica. Tuxtla Gutiérrez, Chiapas, México*

[5]*Departamento de Ingeniería Civil y Ambiental, Universidad de la Costa, Barranquilla, Colombia*

ARTICLE INFO

Article History:
Received 02 January 2020
Revised 15 February 2020
Accepted 17 March 2020

Keywords:
Ciénaga de Mallorquín
Coastal lagoon
Environmental fluid dynamics code (EFDC)
Environmental modeling
Eutrophication
Trophic state index

ABSTRACT

Ciénaga de Mallorquín is a coastal lagoon designated as a RAMSAR site due to its ecological regional and international importance. In this work, the environmental fluid dynamics code explorer modeling system was implemented to determine the spatio-temporal distribution of temperature, dissolved oxygen, chemical oxygen demand and nutrient levels, and assess the trophic status of Ciénaga de Mallorquín. The model was set up with field measurement data taken during transition period and wet season, and secondary information obtained from local authorities and environmental agencies. The results of model simulations were calibrated and verified by the root mean square error method, achieving a consistent fit for all considered variables. Average velocities were between 0.006 m/s and 0.013 m/s during the analyzed periods. The temperature was higher in the wet season than in the transition period (29°C and 31.5°C, respectively). The dissolved oxygen was similar in both periods (6.6 and 6.7 mg/L). NO_3 concentrations were higher during the transition period (3.28 mg/L), with a minimum of 1.76 mg/L and a maximum of 5.09 mg/L. The lowest NO_3 concentrations were found in the area influenced by the connection with the Caribbean Sea. PO_4 concentrations in the wet season were lower than in the transition period (0.20 mg/L). Finally, Ciénaga de Mallorquín exhibits high productivity levels with Trophic State Index > 50 and temporal variations of mesotrophic to eutrophic. The use of Trophic State Index is useful for the management of water body eutrophication and productivity, making it particularly important in aquatic ecosystems.

DOI: 10.22034/gjesm.2020.03.02

NUMBER OF REFERENCES	NUMBER OF FIGURES	NUMBER OF TABLES
61	10	5

*Corresponding Author:
Email: *franklintorres@correo.unicordoba.edu.co*
Phone: +5730 05677648
Fax: +574 7 86 0381

Note: Discussion period for this manuscript open until October 1, 2020 on GJESM website at the “Show Article.

INTRODUCTION

Coastal lagoons are shallow, productive and biologically diverse aquatic ecosystems, which communicate with the ocean through permanent or ephemeral channels and have freshwater inputs (Miranda *et al.,* 2002; Anthony *et al*., 2009). Coastal lagoons provide a wide assortment of ecosystem services (Pérez-Ruzafa *et al.,* 2011; Newton *et al.,* 2018), including their function as buffering zones for materials derived from fluvial input (Kennish and Paerl, 2010), and their role as strategic ecosystems, providing refuge, foraging and breeding habitats for a diversity of species (Panda *et al.,* 2015). Physicochemical properties and ecological productivity in these ecosystems depend on interactions between wind magnitude and direction, tides and fluvial discharge (Panda *et al.,* 2015). Therefore, these ecosystems exhibit spatial and temporal gradients in their physicochemical and ecological features (Contreras and Castañeda, 2004; Pérez-Ruzafa *et al*., 2019). In the same way, the hydrodynamic behavior of coastal lagoons takes part in their function, not only due to their importance in distributing water quality features, but also because of its implications in species connectivity (Pérez-Ruzafa and Marcos, 2012). On the other hand, industrialization, urban development, population growth and diverse anthropogenic activities have modified the concentrations of nutrients, contaminants and sediments discharged into coastal lagoons (Ramesh *et al.,* 2015). These water bodies are probably one of the most vulnerable, transformed and endangered systems on earth, particularly if the effects of climate change are considered (Chapman, 2012). The vulnerability of coastal lagoons to eutrophication processes has become the most relevant problem of these ecosystems (Fertig *et al.,* 2013). Eutrophication results in an increased primary productivity, oxygen depletion (anoxia), high mortality rates among aquatic organisms, and alterations of the trophic chain (Glibert *et al.,* 2010). Several indexes have been employed to determine the trophic state of lakes and coastal lagoons, among which the Carlson Trophic State Index (TSI) (Carlson, 1977; Marreto et al., 2017) is one of the most used. There is an increasing interest in characterizing functional attributes of natural hydrological ecosystems (Newton *et al.,* 2014; Panda *et al.,* 2015; García-Oliva *et al.,* 2018). However, this is a complex task due to the extensive and costly sampling campaigns needed to monitor ecosystem variability and uncertainty, in order to obtain proper, relevant, and reliable information required for decision making (Jones *et al.,* 2001; Velasco *et al.,* 2018). A variety of software packages, as well as numerical solutions for modelling, in the form of "support tools" have been recently developed (García-Oliva *et al.,* 2018; Torres-Bejarano *et al.,* 2019; Liu *et al.,* 2019). These tools allow to represent the characteristics and behavior of relationships within the system from their corresponding predictive analytic capabilities, which are useful to define approaches and manage complex problems related to aquatic resources (Torres-Bejarano *et al.,* 2016). Modelling studies guarantee a holistic approach to understand trophic dynamics in tropical, shallow water coastal ecosystems (Itoh *et al.,* 2018). In this regard, the Environmental Fluid Dynamics Code (EFDC) model has become one of the most widely used hydrodynamic and water quality models. The EFDC Explorer model demonstrates its friendliness to data pre-processing, high performance computing, numerical robustness and post-processing capacity. Plus, it has been applied and successfully implemented in several study cases worldwide (Luo and Li, 2009; Shin *et al.,* 2019). Previous research has employed the EFDC model to study the hydrodynamics and to simulate the distribution of salinity, temperature, nutrients, and dissolved oxygen (DO), as well as to simulate the hypoxia in response to the changing local hydrological and climatological variables (Xia *et al*., 2011; Devkota *et al*., 2013; Xia and Jiang, 2015). The seasonal and dynamic of water quality has been a focus in the last decade, due to the trends of more sophisticated management (Jiang *et al*., 2019). However, little information is available on the physicochemical and ecological function of heavily intervened and modified coastal lagoons. Therefore, this study aimed to determine the hydrodynamic and spatial-temporal distribution of water quality parameters (temperature, dissolved oxygen (DO), chemical demand of oxygen (COD), nitrates and phosphorus), and determine the trophic state using EFDC Explorer model in the Ciénaga de Mallorquín, which is a coastal lagoon located in northern Colombia, with influence of the Caribbean Sea. The field measurements and model simulations were carried out in transition (June) and wet (September) seasons of 2015.

MATERIALS AND METHODS

Description of the study area and context

Ciénaga de Mallorquín (74°52'00''W, 11°05'00''N) is located in the northeast portion of the Atlántico department of Colombia (Fig. 1). It is the only estuarine coastal lagoon in northern Colombia, and globally relevant as part of the RAMSAR site of the estuarine delta system of the Magdalena River, Ciénaga Grande de Santa Marta (the second largest in Colombia with 400.000 ha) (Galvis *et al.,* 1992). The lagoon bounds to the north with the Caribbean Sea, and they interchange water sporadically, through a connection that sometimes is natural and sometimes artificial. To the east the lagoon limits with the Magdalena River through two box culverts lying across the west breakwater, and to the west it limits with the mouth of Arroyo León stream, which supplies a significant volume of freshwater during the annual wet season. In 1936, west and east breakwaters (7.4 and 1.4 km, respectively) were built to avoid sedimentation and promote commercial navigation to the Port of Barranquilla, resulting in significant morphological change of the Magdalena River estuarine delta system. After the breakwaters were built, different processes led to the disappearance of several bars that separated four lagoons belonging to the Magdalena River delta flood complex, merging into a single lagoon (Ciénaga de Mallorquín). Major alteration of the water body started in 1940, mainly due to interruption of the water interchange needed to maintain ecosystem function. On the other side, stilt houses have been built without connections to the sewage network, spilling waste directly into water bodies in the area (Magdalena River, Arroyo Leon stream and Ciénaga de Mallorquín) (Garcés-Ordóñez *et al.,* 2016a). Nevertheless, communities inhabiting the area use the lagoon for consumption, fishing and transportation (Arrieta and de la Rosa, 2003). In general terms, Ciénaga de Mallorquín is a shallow water body (1.1 m average depth). It is surrounded by floodplains, sandy areas and dunes, and mangroves are present (Galvis *et al.,* 1992). Turbidity is 60 NTU, average water temperature is 28.40 °C, and salinity exhibits spatial and seasonal fluctuations, ranging from 2 to 34, with an average of 15.1 (Arrieta and de la Rosa, 2000). Due to the strong anthropogenic pressure and climate change effects, Ciénaga de Mallorquín has suffered dramatic variation of its water surface, losing approximately 650 ha between 1980 and 2010. This is equivalent to 43.18% of area loss, roughly half of the lagoon, and resulted in increased erosion of foreshores, sand bars and mangrove areas. Shoreline retreat is in the order of 2,200 m (Arrieta and de la Rosa, 2003). Weather in the study area is strongly influenced by oscillations of the Intertropical Convergence Zone (ITCZ), with two identifiable periods, a dry season from January to April, and a wet season from August to December (Poveda, 2004). The lapse between May and July is considered a transition period (Poveda, 2004). Northeast trade winds are the most influential in the study area, with a prevailing northern direction (Andrade, 2001). Precipitation and evaporation rates are 835.50 mm and 1,948.90 mm, respectively (Poveda, 2004).

Data collection and laboratory analysis

Measurements and sampling were performed in two field campaigns, one in the transition period (June 2015) and other during the wet season (September 2015). Two monitoring points in Ciénaga de Mallorquín (Fig. 1) were selected in order to use these data for model calibration. In situ salinity, temperature and DO measurements were taken with a multiparameter sonde (YSI 600 Pro-Plus). In addition, surface water samples were collected with a Niskin bottle. Water samples were preserved in amber glass bottles at 4°C and transported to the laboratory (Quamrul *et al.,* 2016). COD and nutrient (nitrate and phosphate) concentrations were determined by colorimetric analysis (Parson *et al.,* 1984). Bathymetric and hydrodynamic measurements of the study area were taken from a boat, along transects from one shore to the other of the lagoon; a RiverRay RD-I Acoustic Doppler Current Profiler (ADCP), at 600 KHz, was employed. The ADCP allows measuring the velocity and direction of the water column. The profiler was operated with the software WinRiver II (v. 10.0), through simultaneous, coordinated integration of the bathymetric sonde (Garmin-Echomap 73sv) and the GPS (Garmin). This integration produced files with information on current magnitude and direction, velocity profiles, geographic location (latitude - longitude) and depth of measurements.

Additional information

Together with field measurements, additional secondary information was compiled for calibration

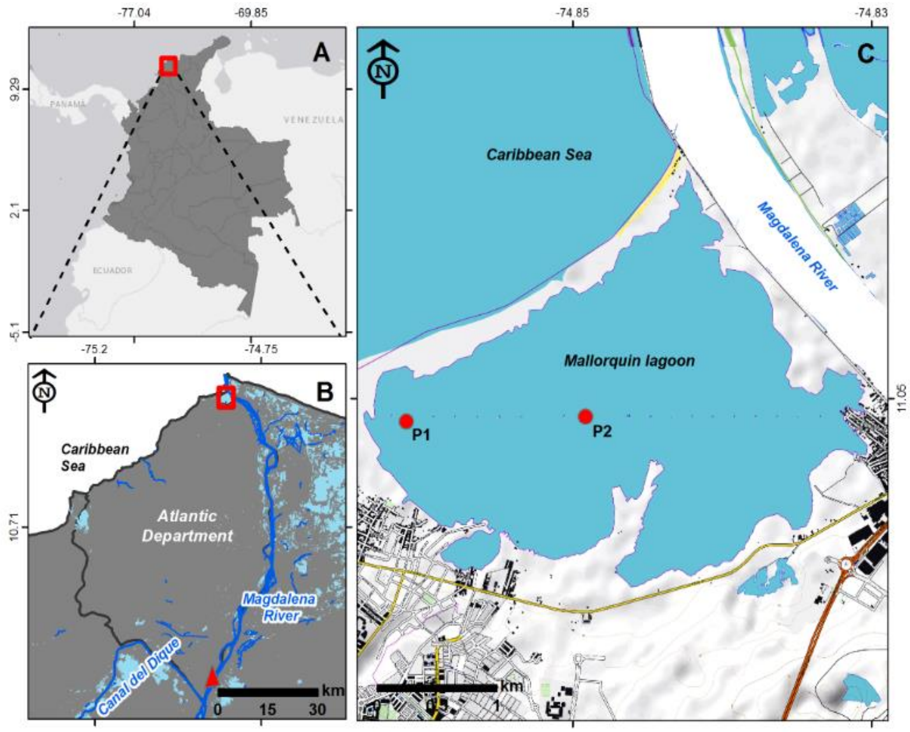

Fig. 1: Geographic location of the study area along with the measurement stations used in the calibration process (P1 and P2).

and validation of the EFDC model. Information on water quality and environmental data (technical historical reports) was obtained from the local environmental authority Regional Autonomous Corporation (CRA) of the Atlántico department. Surveys in four points of Ciénaga Mallorquín were performed by CRA for five contiguous days within two climatic period (transition and wet seasons) of the same year monitoring physicochemical, microbiological and hydrobiological water quality parameters of main water bodies of the Atlántico Department, available through the Water Resource Information System. In addition, meteorological data for the study area (precipitation regimes, evaporation, temperature, relative humidity, wind speed and direction) was compiled from the Colombian Institute of Hydrology, Meteorology and Environmental Studies (IDEAM). Tide data were obtained from the Caribbean Oceanographic and Hydrographic Research Institute (CIOH).

Description of the numerical model

The EFDC model was originally developed at the Virginia Institute of Marine Science and later sponsored by the US Environmental Protection Agency (US EPA). This is a hydrodynamic and water quality model that can be applied to any surface water body, including lakes, rivers and estuaries (Hamrick, 1992). The EFDC structure is characterized by a) a finite-difference cell-based model, b) the ability of wetting and drying during contour processing, c) allowing heat interchange with the atmosphere and d) simulate water quality (Wang *et al.,* 2013). The EFDC solves the Navier-Stokes equations for hydrodynamic studies, adapted for shallow waters, and solves the Advection-Diffusion-Reaction equations for contaminant transport or water quality studies (Hamrick, 1992; Devkota *et al*., 2013; Zhang *et al*., 2017). The EFDC Explorer 8.2 version, is a comprehensive and flexible tool designed for the EFDC modelling system, which was optimized by Dynamic Solutions-International company (DSI), who developed an user interface that makes friendly the implementation of the model, from data pre-processing to results post-processing and analysis (Devkota *et al*., 2013).

Hydrodynamic module

The EFDC hydrodynamic module of the model solves 3D, vertically hydrostatic, free surface, and turbulent averaged equations of motion for a variable-density fluid. Dynamically coupled transport equations for turbulent kinetic energy, turbulent length scale, salinity, and temperature are also solved. The model solves the Eqs. of motion 1 and 2, the continuity Eq. 3, the UNESCO's equation of state Eq. 4 (UNESCO, 1981), and the transport Eqs. 5 and 6 for salinity and temperature. All these equations are vertically integrated. It uses cartesian or curvilinear orthogonal horizontal coordinates, as well as a sigma coordinate system in the vertical dimension (Hamrick, 1992; Tetra Tech, 2007; Ji, 2017).

$$\overbrace{\frac{\partial(m_x m_y Hu)}{\partial t}}^{1} + \overbrace{\frac{\partial(m_y Huu)}{\partial x} + \frac{\partial(m_x Hvu)}{\partial y} + \frac{\partial(m_x m_y wu)}{\partial z}}^{2} - \overbrace{\left(m_x m_y f + v\frac{\partial m_y}{\partial x} - u\frac{\partial m_x}{\partial y}\right)Hv}^{3} = \overbrace{-m_y H\frac{\partial(g\zeta + p)}{\partial x}}^{4} - \overbrace{m_y\left(\frac{\partial h}{\partial x} - z\frac{\partial H}{\partial x}\right)\frac{\partial p}{\partial z} + \frac{\partial}{\partial z}\left(m_x m_y \frac{1}{H} A_V \frac{\partial u}{\partial z}\right)}^{5} + Q_u \quad (1)$$

$$\overbrace{\frac{\partial(m_x m_y Hv)}{\partial t}}^{1} + \overbrace{\frac{\partial(m_y Huv)}{\partial x} + \frac{\partial(m_x Hvv)}{\partial y} + \frac{\partial(m_x m_y wv)}{\partial z}}^{2} + \overbrace{\left(m_x m_y f + v\frac{\partial m_y}{\partial x} - u\frac{\partial m_x}{\partial y}\right)Hu}^{3} = \overbrace{-m_x H\frac{\partial(g\zeta + p)}{\partial y}}^{4} - \overbrace{m_x\left(\frac{\partial h}{\partial y} - z\frac{\partial H}{\partial y}\right)\frac{\partial p}{\partial z} + \frac{\partial}{\partial z}\left(m_x m_y \frac{1}{H} A_V \frac{\partial v}{\partial z}\right)}^{5} + Q_v \quad (2)$$

$$\frac{\partial(m_x m_y \zeta)}{\partial t} + \frac{\partial(m_y Hu)}{\partial x} + \frac{\partial(m_x Hv)}{\partial y} + \frac{\partial(m_x m_y w)}{\partial z} = 0 \quad (3)$$

$$\rho = \rho(p,S,T) = 999.842594 + 6.793952\times10^{-2}T - 9.095290\times10^{-3}T^2 + 1.001685\times10^{-4}T^3 - 1.120083\times10^{-6}T^4 + 6.536332\times10^{-9}T^5 + \begin{pmatrix}0.824493 - 4.0899\times10^{-3}T + 7.6438\times10^{-5}T^2 \\ -8.2467\times10^{-7}T^3 + 5.3875\times10^{-9}T^4\end{pmatrix}\cdot S + \begin{pmatrix}-5.72466\times10^{-3} + 1.0227\times10^{-4}T - \\ 1.6546\times10^{-6}T^2\end{pmatrix}\cdot S^{1.5} + 4.8314\times10^{-4}S^2 \quad (4)$$

$$\frac{\partial(mHS)}{\partial t} + \frac{\partial(m_y HuS)}{\partial x} + \frac{\partial(m_x HvS)}{\partial y} + \frac{\partial(mwS)}{\partial z} = \frac{\partial}{\partial z}\left(m\frac{1}{H}A_b\frac{\partial S}{\partial z}\right) + Q_S \quad (5)$$

$$\frac{\partial(mHT)}{\partial t} + \frac{\partial(m_y HuT)}{\partial x} + \frac{\partial(m_x HvT)}{\partial y} + \frac{\partial(mwT)}{\partial z} = \frac{\partial}{\partial z}\left(m\frac{1}{H}A_b\frac{\partial T}{\partial z}\right) + Q_T \quad (6)$$

Where *u,v* are the horizontal velocity components in the curvilinear coordinates; *x,y* are the orthogonal curvilinear coordinates in the horizontal direction; *z* is the sigma coordinate; m_x, m_y are the square roots of the diagonal components of the metric tensor "m"; $H = h+\zeta$, Total depth, is the sum of depth and free surface; *p* is the physical pressure in excess of the reference density hydrostatic pressure; *f* is the Coriolis parameter; A_v is the vertical turbulent eddy viscosity; Q_u, Q_v are momentum source-sink terms; *ρ* is the water density; *T* is the water temperature; *S* is the water salinity; A_b is the vertical turbulent diffusivity; Q_S, Q_T horizontal diffusion and thermal sources and sinks.

Pollutants transport module

The eutrophication model in the EFDC solves mass balance equations for 21 variables in the water column. These variables include diverse Carbon, Nitrogen and Phosphorus components, as well as Silica cycles, Dissolved Oxygen dynamics, three groups of algae, and fecal coliforms (Hamrick, 1992).

The mass balance equation for each of the water quality state variables can be expressed as Eqs. 7.

$$\overbrace{\frac{\partial}{\partial t}(m_x m_y HC)}^{1} + \overbrace{\frac{\partial}{\partial x}(m_y HuC) + \frac{\partial}{\partial y}(m_x HvC) + \frac{\partial}{\partial z}(m_x m_y wC)}^{2} + \overbrace{\frac{\partial}{\partial z}(m_x m_y w_{sc} C)}^{3} = \overbrace{\frac{\partial}{\partial x}\left(\frac{m_y}{m_x}HA_H\frac{\partial C}{\partial x}\right) + \frac{\partial}{\partial y}\left(\frac{m_x}{m_y}HA_H\frac{\partial C}{\partial y}\right) + \frac{\partial}{\partial z}\left(\frac{m_x m_y}{H}A_b\frac{\partial C}{\partial z}\right)}^{4} + \overbrace{S_c}^{5} \quad (7)$$

C is the concentration or intensity of transport constituent; *u,v* are the horizontal velocity components in the curvilinear coordinates; *w* is the vertical velocity component; A_H is the horizontal turbulent eddy diffusivity; A_b is the vertical turbulent eddy diffusivity; S_c is the internal and external sources and sinks per unit volume; *H* is the total water depth; w_{sc} is a positive settling velocity when *C* represents a suspended material; S_c is the source/sink term for the constituent. Water temperatures are needed for computation of the water quality state variables, and they are provided by the internally coupled hydrodynamic model (Park *et al.*, 2005). Details about EFDC model structure for water quality and eutrophication processes can be found in (Tetra Tech, 2007; Zou *et al.*, 2014; Ji, 2017).

Numerical solution scheme

To solve the equations of motion in EFDC model, a numerical scheme of finite second order precision differences in space is used, on a Staggered Cell or MAC type grid. The temporal integration of the model follows a second order finite difference scheme, with an internal-external division procedure to separate the baroclinic mode of the gravity wave from the external free surface, or barotropic mode. The external solution mode is semi-implicit and simultaneously calculates the two-dimensional surface elevation field using a preconditioned conjugate gradient procedure. The external solution is completed by calculating the barotropic velocities averaged at depth, using the new surface elevation field. The semi-implicit external solution of the model allows large time steps, which are limited only by stability criteria of the explicit advection scheme in centered differences or the upwind scheme, used for nonlinear accelerations (Tetra-Tech, 2007). The horizontal boundary conditions for the external solution mode offer options to simultaneously specify the elevation of the free surface directly, the characteristic of an incoming wave, the free radiation of an output wave, or the normal volumetric flow over arbitrary portions of border. Additionally, the EFDC model implements a second-order fractional step mass conservation solution schema in space and time for Eulerian transport equations, at the same time step or twice the time step of the solution of the equation of motion. The advective step of the transport solution uses either the centered difference scheme used in the Blumberg-Mellor model or an upstream hierarchical difference scheme (Tetra-Tech, 2007; Jeong *et al.*, 2010). The horizontal diffusion step is explicit in time, while the vertical diffusion stage is implicit.

Table 1: Trophic State Index (TSI) (Carlson, 1977)

Range	Trophic State
0 < TSI≤30	oligotrophic
30 < TSI ≤40	oligo-mesotrophic
40 < TSI≤50	mesotrophic
50 < TSI≤60	slightly eutrophic
60 < TSI≤70	moderately eutrophic
70 < TSI	hypereutrophic level

Eutrophication by EFDC Explorer

Eutrophication is assessed through trophic state indexes. The Trophic State index (TSI), which varies between 0 and 100 (Table 1), is one of the most widely used to determine the trophic state of an ecosystem (Carlson, 1977). This index is calculated by EFDC from other parameters, such as total phosphorus (Zhang and You, 2017; Luo and Li, 2018).

Model configuration

A numerical grid must be designed for free surface modelling, allowing to determine flux variable values (velocity for hydrodynamics and concentrations for pollutant transport) for each element (cell) in the Cartesian coordinate system. The numerical grid used for Ciénaga de Mallorquín had a uniform spacing, with ΔX=ΔY=15 m, 294 elements in the X axis and 384 elements in the Y axis, for a total of 112,896 elements, of which 30,922 were active cells. Bathymetry of the study area exhibited depths between 0 and 3.50 m, with an average depth of 1.12 m. The deepest zones are the result of dredging, performed by

Table 2: Tidal constituents, amplitude and phase at Mallorquín-Sea mouth.

Name	Speed (deg/h)	Amplitude (m)	Phase (deg)
Q1	13.3987	0.0058	0.8070111
O1	13.943	0.0615	0.9169846
P1	14.9589	0.0313	1.013632
K1	15.0411	0.0945	0.9896625
N2	28.4397	0.0208	0.8605379
M2	28.9841	0.0497	1.09101
S2	30	0.015	0.3333333
K2	30.0821	0.0041	0.5214231

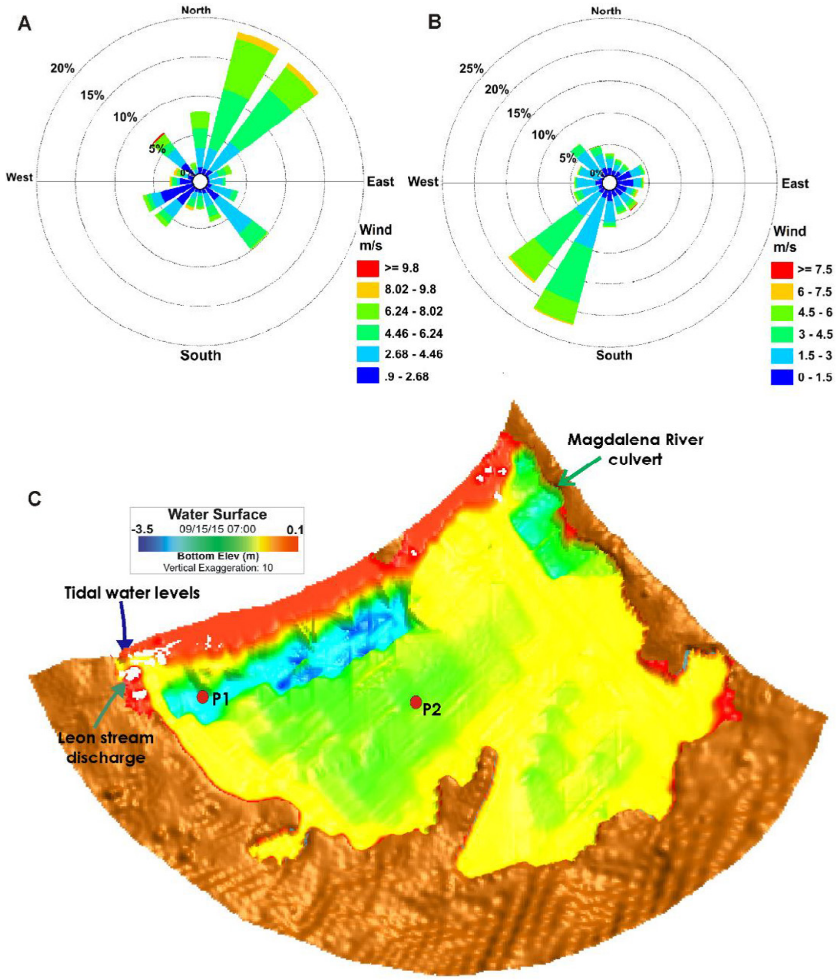

Fig. 2: A) Wind roses at Ernesto Cortissoz airport station for transition period. B) Wind roses at Ernesto Cortissoz airport station for wet season. C) Bathymetry, boundary conditions and control points.

environmental authorities to create sediment traps in the inputs of sea water and freshwater.

Forcing and boundary conditions

For the study area wind forcing data are used, Arroyo León (flow) discharge, connections with the Magdalena river through box-culverts and tide variations for the coastal zone. In this work, the connection between Ciénaga de Mallorquín and the Caribbean Sea was only present in wet season and was artificially built by fishermen near to the mouth of Arroyo León stream (Fig. 2), so two simulation scenarios were established: one with the lagoon-sea connection (wet season) and the other without this connection (transition season).

Input conditions employed for hydrodynamic simulation are shown in Table 3. The highest freshwater input to the lagoon is the entrance of Arroyo León stream (4.50 m^3/s during the transition period and 6 m^3/s during the wet season). Table 4 shows input data employed for water quality simulation of Arroyo León, the Magdalena River, Ciénaga de Mallorquín, and the incoming tide.

Model validation

The water quality model was validated by comparing the monitoring data with the simulation data of Ciénaga de Mallorquín at the two measurements/control points (Fig. 2) in June and September 2015. The model was initially run

Table 3: Input data and key parameters for hydrodynamic module.

Parameter	Value	
Manning Coefficient	0.025	
Timestep, Δt (s)	1.0	
Background horizontal eddy viscosity (m^2/s)	0.25	
Dimensionless horizontal momentum diffusivity	0.0025	
Background vertical eddy viscosity (m^2/s)	0.00001	
Vertical molecular diffusivity (m^2/s)	1×10−9	
	Transition	Wet
Leon stream flow (m^3/s)	4.5	6
Magdalena River flow (m^3/s)	0.65	0.85

Table 4: Data concentrations for water quality simulation

	León stream		Magdalena River		Mallorquín lagoon		Tidal water inlet	
Parameter	Transition	Wet	Transition	Wet	Transition	Wet	Transition	Wet
T (°C)	31.30	30.30	30.50	31.20	31.20	31.6	28	31
Salinity	9	16	7	7	7	15.1	NA	35
DO (mg/L)	4.80	9.80	3.60	6.40	5.20	8.46	6.80	9.70
COD (mg/L)	18.75	18.50	20	20.10	19.13	19.5	13	13.20
NO3 (mg/L)	1.98	1.92	3.06	3.06	1.06	1.34	1.30	2.80
PO_4 (mg/L)	0.24	0.228	0.36	0.36	0.30	0.21	0.24	0.24

NA: Not applicable.

Table 5: Main coefficients and constants of the water quality model.

Parameter	Value
Reaeration rate constant	0.80/day
COD decay rate	0.00038/day
Oxygen Half-saturation Constant for COD Decay	1 mg O_2/L
Maximum nitrification rate	0.50/day
Minimum hydrolysis rate of refractory particulate organic phosphorus	0.007/day
Minimum hydrolysis rate of labile particulate organic phosphorus	0.08/day
Minimum hydrolysis rate of dissolved organic phosphorus	0.10/day
Minimum hydrolysis rate of refractory particulate organic nitrogen	0.005/day
Minimum hydrolysis rate of labile particulate organic nitrogen	0.075/day
Minimum Mineralization Rate of dissolved organic nitrogen	0.015/day
Maximum growth rate for algae	1.90/day
Basal metabolism rate for algae	0.04/day
Nitrogen half-saturation for algae growth	0.01 mg N/L
Phosphorus half-saturation for algae growth	0.001 mg P/L

with the default and available values in the EEMS software for water quality variables (reaction coefficients, constants and sedimentation rates, etc.), subsequently, those coefficients were adjusted until reaching reasonable agreement between simulation data and observed data, always in agreement with the references values reported in related literature and similar studies (Table 5). To verify the quality of the numerical solution with respect to observed data, EFDC model results were evaluated using the root mean square error (RMSE) method, to confirm that simulated results were consistent and in accordance with observed values (McCuen *et al.,* 2006; Zhang and You, 2017).

RESULTS AND DISCUSSION

Calibration model

A comparison between field measured velocity vectors (red arrows) and those calculated by the model (black arrows) is shown in Fig. 3. Modelling

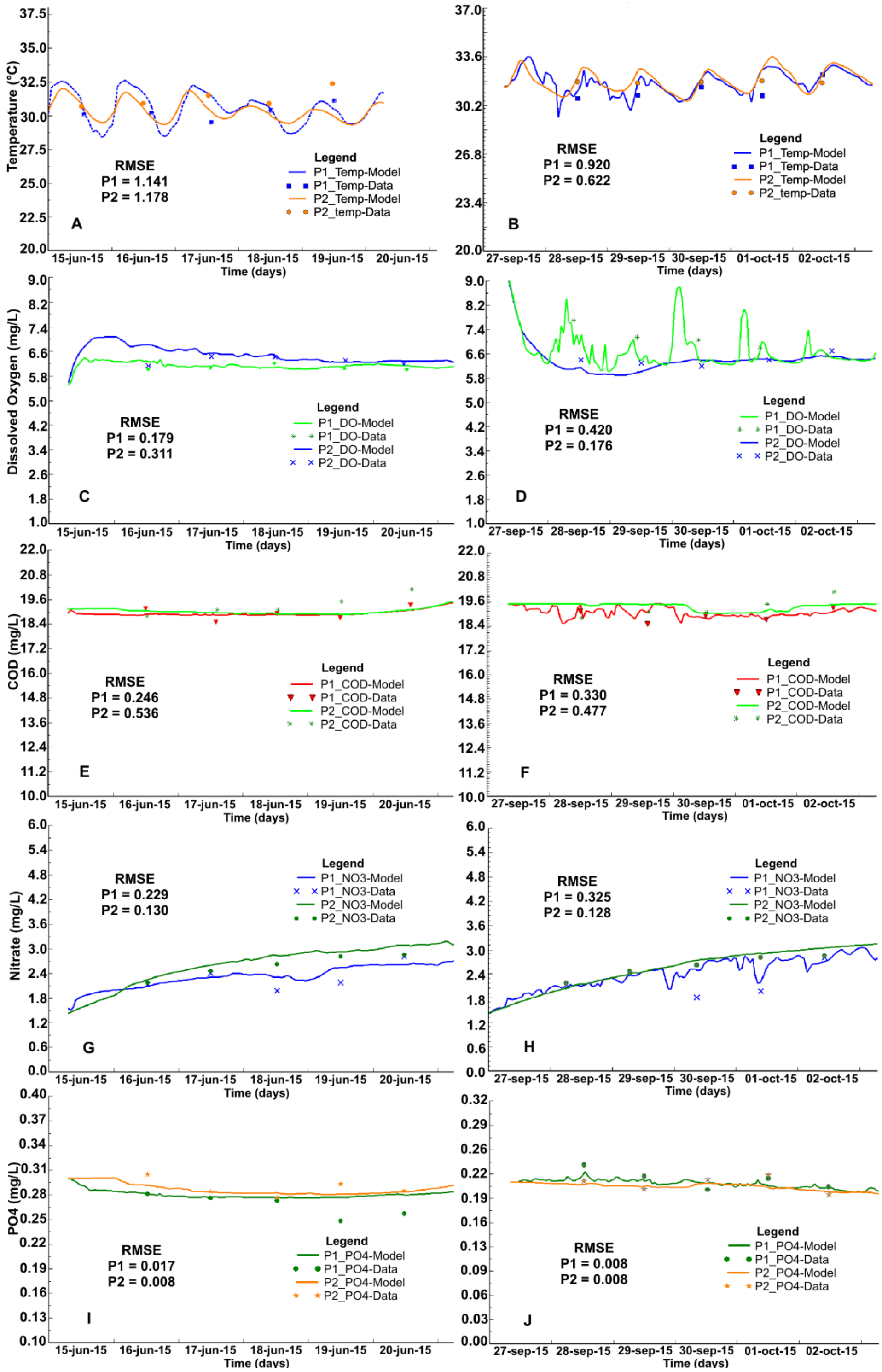

Fig. 3: Hydrodynamic validation and calibration water quality parameters. A) Temperature for the transition period. B) Temperature for the wet season. C) DO for the transition period. D) DO for the wet season. E) COD for the transition period. F) COD for the wet season. G) NO_3 for the transition period. H) NO_3 for the wet season. I) PO_4 for the transition period. J) PO_4 for the wet season

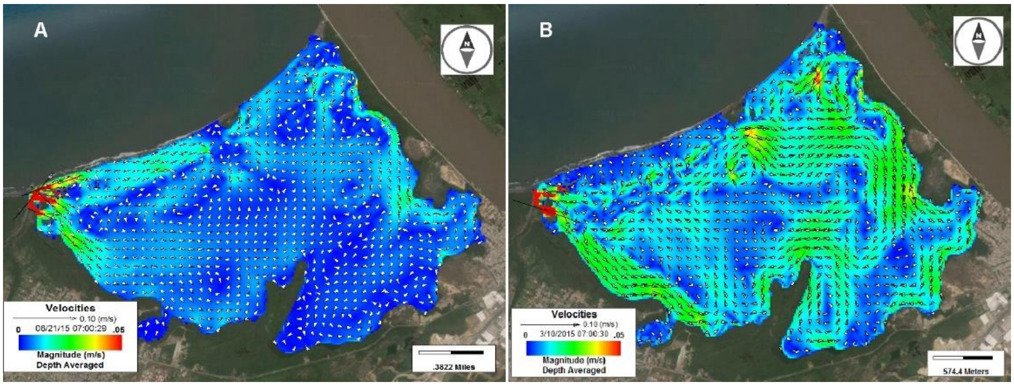

Fig. 4: Hydrodynamics simulation for Mallorquín Lagoon. A) Transition Period. B) Wet season.

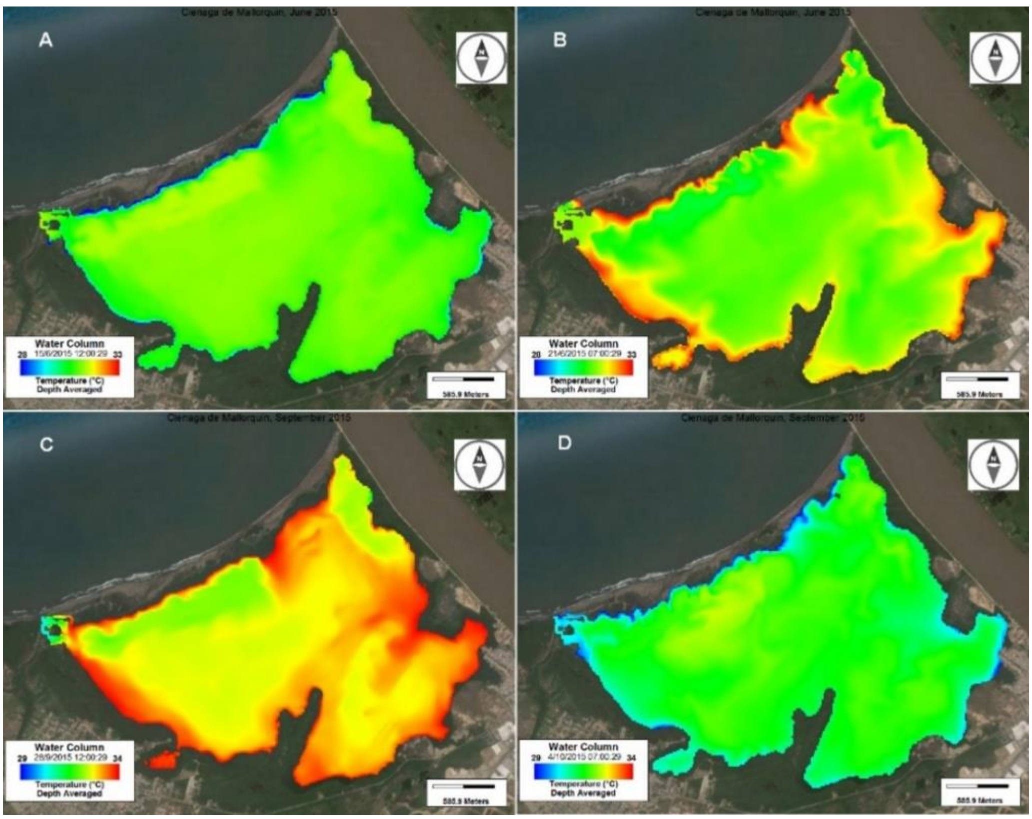

Fig. 5: Simulation of temperature variation. A) Transition Period (0.5 days of simulation). B) Transition Period (6 days of simulation). C) Wet season (0.5 days of simulation). D) Wet season (6 days of simulation) (wet season: note the change in scale values).

results show a good fit for both direction and magnitude. Therefore, processes related to boundary conditions (flow input and output) and atmospheric balance can be considered as properly established. This result allows implementing the model under different scenarios, in this case, different climatic conditions leading to different discharge levels. The calibration results for the water quality variables are displayed in Fig. 3. The statistic values show an excellent correlation and fit between simulated and

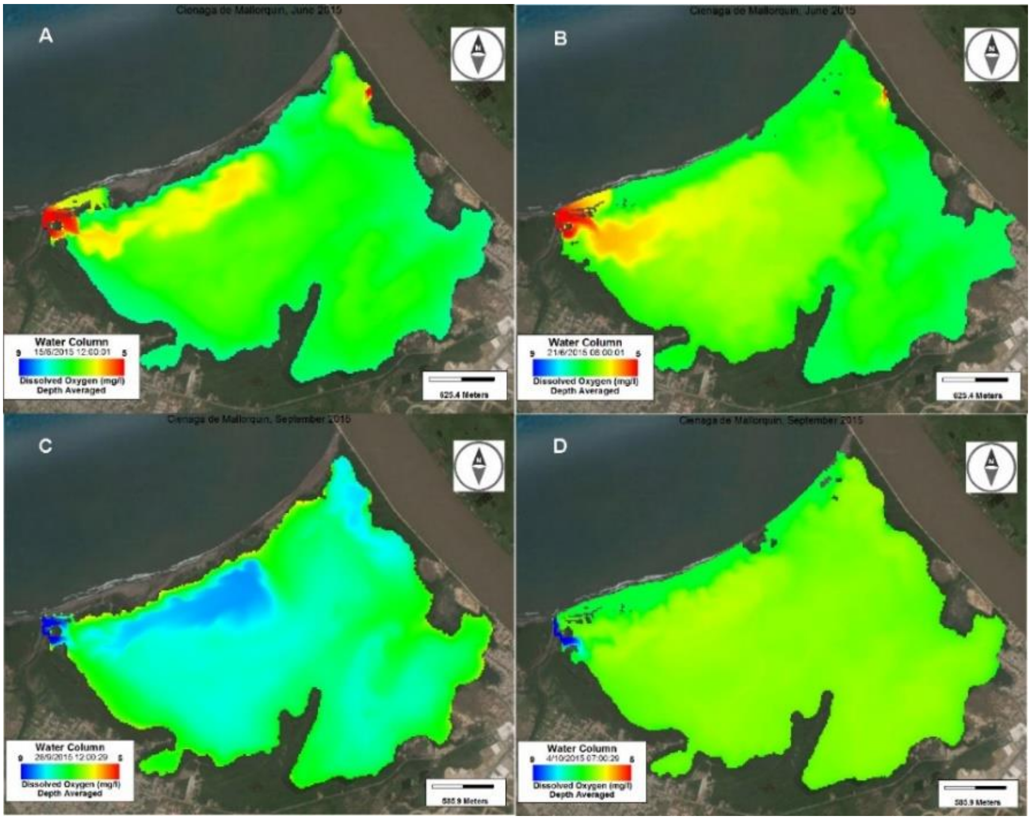

Fig. 6: Simulation of DO variation. A) Transition Period (0.5 days of simulation). B) Transition Period (6 days of simulation). C) Wet season (0.5 days of simulation). D) Wet season (6 days of simulation) (wet season: note the change in scale values)

in situ observed variables. In other words, results of the model are consistent with measurements in both time periods (Fig. 3).

Hydrodynamic simulation

Resulting velocities values obtained by the model for the transition period are shown in Fig. 4A. Under these simulation conditions average velocities of 0.006 m/s and maximum velocities of 1.050 m/s were observed. On the other hand, Fig. 4B shows the velocities values obtained for the wet season. Under these simulation conditions, average observed velocity was 0.013 m/s, with a maximum of 1.165 m/s. In both cases, maximum velocities were close to Arroyo León discharge, Magdalena River connection through box culvers, and close to the connection with the Caribbean Sea. However, due to the low water flow, these do not represent a significant influence on circulation patterns within the lagoon, and their effect is primarily local. The hydrodynamic behavior of Ciénaga de Mallorquín displays three main recirculation zones. Some current patterns in the form of vortices are observed in the central zone of the lagoon and West-East-West currents occurring during most of the simulation period, favoring flux-ebb, as well as dissolved and suspended material transport, and promoting water renewal.

Water velocity values were low in both simulated periods, particularly during the transition period, which might be related to wind patterns. The study area is strongly influenced by northeast trade winds, which are affected by the ITCZ movement (Andrade, 2001). Torres-Bejarano *et al*. (2016) reported winds as the main forcing of Ciénaga de Mallorquín dynamics. In addition, seasonal changes in wind magnitude and direction have been shown to cause large scale changes in tropical coastal lagoon circulation (Panda, 2015). The role of wind in turbulence generation is more important at the central portion of these ecosystems, where tide-induced fluxes have no relevance (Cioffi *et al.,* 1995).

Water quality simulation

Temperature

Temperature simulations showed an average temperature of 29°C during the transition period, with a minimum of 27°C and a maximum of 30.5°C. Temperature behavior over 6 days of simulation are shown in Fig. 5 (A and B). Temperature differed among simulation days, with higher temperatures at the sixth day of the simulation, particularly at the coastal border of the lagoon. During the first days of simulation, the lowermost observed temperatures were in the limit with the coastal zone. On the other hand, the wet season showed a different behavior, with an average temperature of 31.5°C, a maximum of 27.6°C and a minimum of 32.5°C (Fig. 5), whereas the highest temperatures were registered during the first day of simulation. For the sixth day of simulation the lowest temperatures were in the coastal border of the lagoon.

Changes in air temperature have a strong influence on the water temperature of shallow, slow-moving water bodies such as coastal lagoons (Anthony *et al.,* 2009). In this work, the lowest temperatures were registered in the central zone of the lagoon, gradually increasing towards the shores, where water is shallower. At lower depths there is greater penetration of solar radiation and greater heat interchange with the atmosphere (Harley *et al.,* 2006). On the other side, the obtained results indicate that Arroyo León stream discharge and tide flux, in both studied time periods, did not have a significant influence on the thermal behavior of the lagoon. Water temperature is one of the most important parameters in coastal lagoons, as it directly influences DO concentrations, as well as organism physiology and distribution (Woodward, 1987). As water temperature increases, it is very likely that DO concentrations will decrease (Joos *et al.,* 2003).

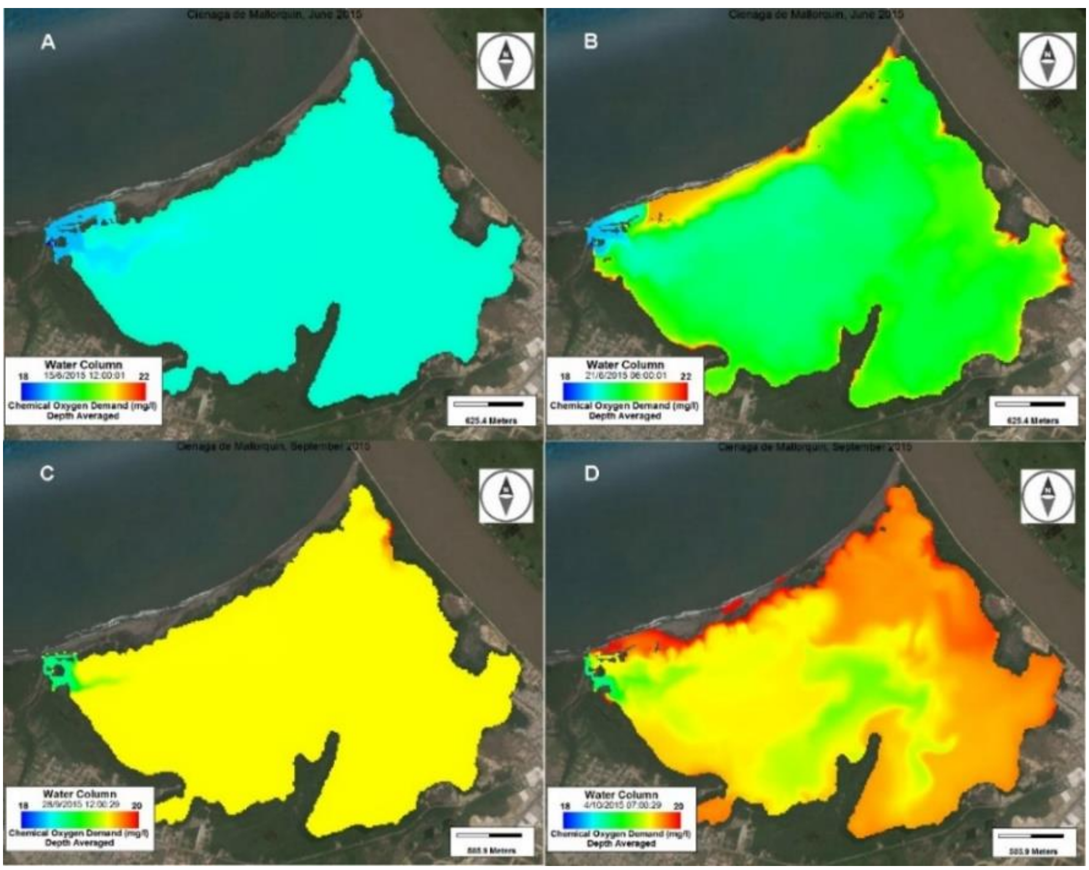

Fig. 7: Simulation of COD variation. A) Transition Period (0.5 days of simulation). B) Transition Period (6 days of simulation). C) Wet season (0.5 days of simulation). D) Wet season (6 days of simulation) (wet season: note the change in scale values)

Dissolved oxygen (DO) and chemical oxygen demand (COD)

For the transition period, average DO was 6.7 mg/L, with a maximum concentration of 9.1 mg/L and a minimum of 4.2 mg/L. DO concentration exhibited a high variability during the 6 days of simulation (Fig. 6). The highest concentrations were reached at the border limiting with the coastal zone and the mouth of Arroyo León. For wet season, average DO concentration levels were 6.6 mg/L, with a maximum of 9.8 mg/L and a minimum of 6.4 mg/L (Fig. 6). The lowest DO concentrations were registered on the first day of simulation, particularly in the zone influenced by the mouth of Arroyo León stream. In the fourth to sixth days of simulation, most of the lagoon area showed DO concentrations close to 3 mg/L, excepting the coastal border with the Caribbean Sea. Average COD during the transition period was 19.86 mg/L, with a maximum concentration of 35.8 mg/L and a minimum of 16.67 mg/L (Fig. 7). Spatial variation was observed during the 6-day simulation period. During the four first days of simulation, the lowest concentrations were observed in the area influenced by Arroyo León. On the sixth day of simulation, a considerable increase of concentrations was observed, particularly in the coastal border of the lagoon, with the highest concentrations in the east and west zones. For the wet season, average COD was 19.57 mg/L, with a minimum of 18.75 mg/L and a maximum of 21.87 mg/L (Fig. 7). The spatial pattern was like that found during the transition period, with the lowest concentrations close to the influence area of Caribbean Sea connection. Likewise, the highest concentrations were found in the south and east parts of the lagoon, at the sixth day of simulation.

DO is the main indicator of environmental state and health in water bodies (Hull *et al.,* 2000). It is an indispensable element for the development of

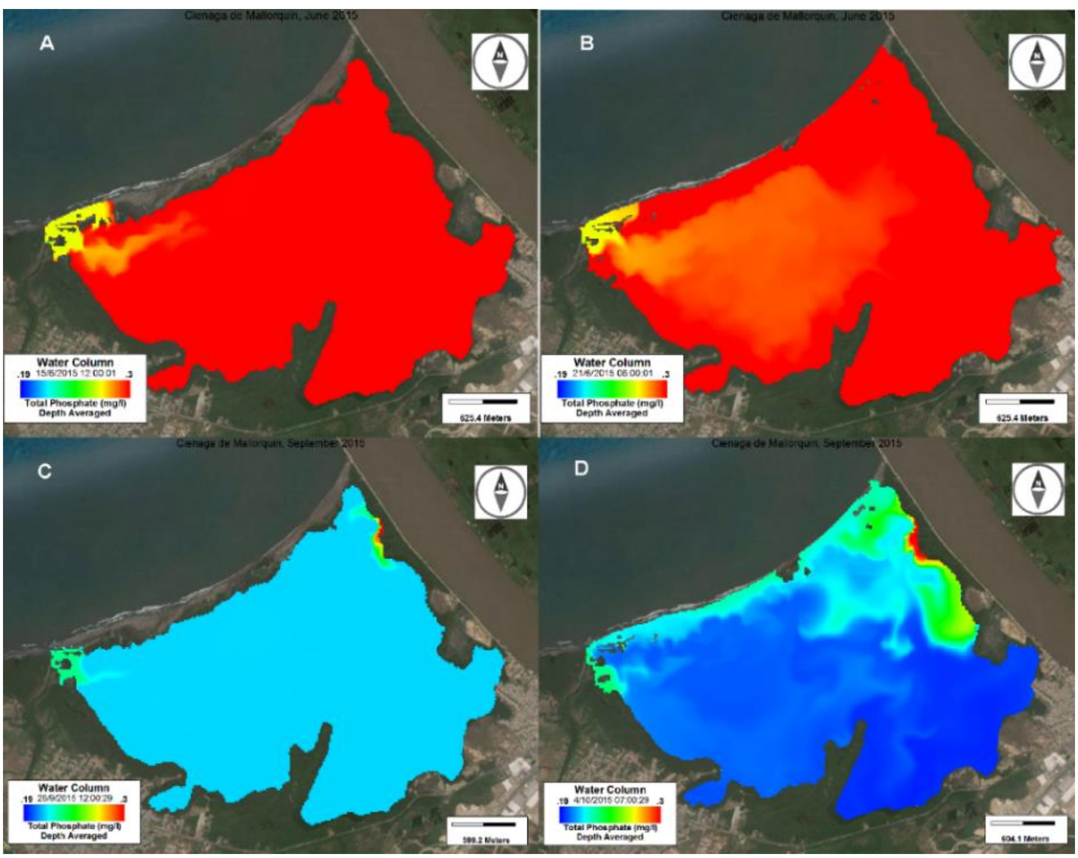

Fig. 8: Simulation of NO_3 variation. A) Transition Period (0.5 days of simulation). B) Transition Period (6 days of simulation). C) Wet season (0.5 days of simulation). D) Wet season (6 days of simulation) (wet season: note the change in scale values).

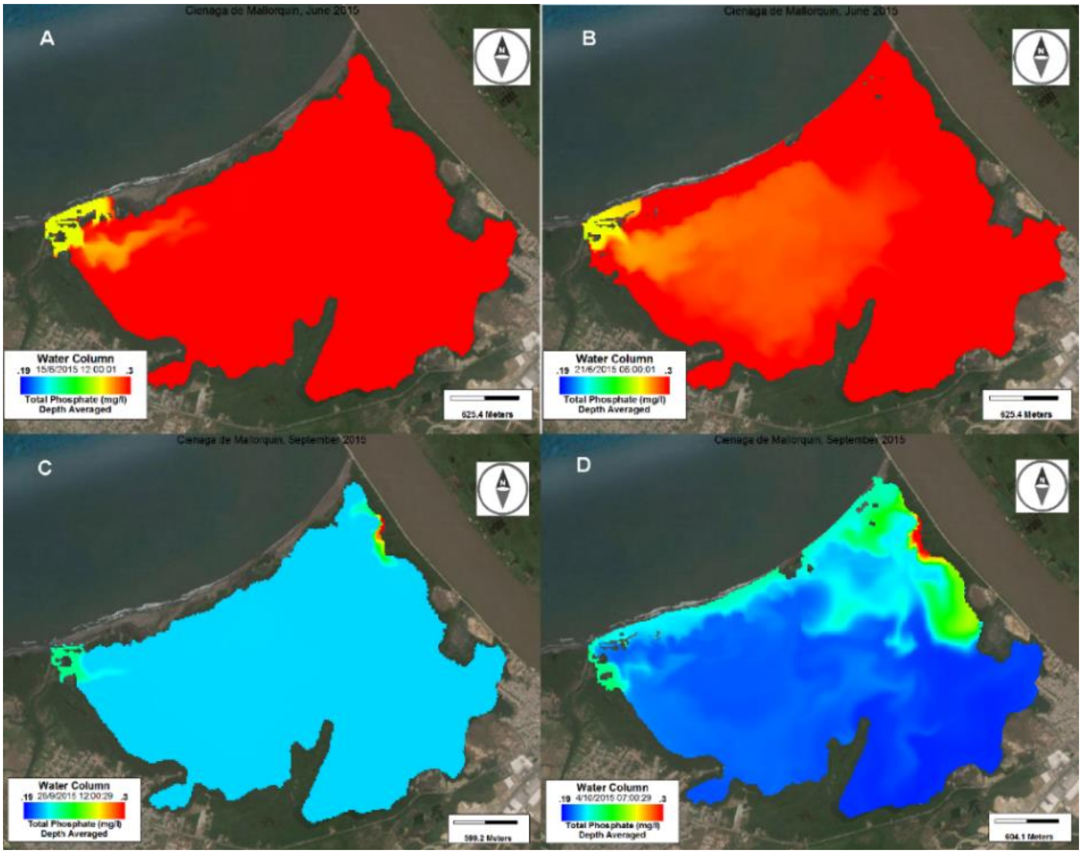

Fig. 9: Simulation of PO^4 variation. A) Transition Period (0.5 days of simulation). B) Transition Period (6 days of simulation). C) Wet season (0.5 days of simulation). D) Wet season (6 days of simulation) (wet season: note the change in scale values).

diverse essential processes in the behavior of aquatic ecosystem, and a decrease below recommended levels may significantly alter ecological equilibrium (Jiménez *et al.,* 2003). For its part, COD quantifies the amount of oxygen required to oxidize the organic matter present in the ecosystem (Hur *et al.,* 2010). This parameter is of major ecological relevance, as the presence of high COD may indirectly reflect conditions close to anoxia (Hur *et al.,* 2010). A clear correspondence between DO and COD was observed in Ciénaga de Mallorquín, that is, when COD diminished, DO concentrations increased. In average, DO concentrations were in the range accepted by Colombian laws for aquatic life preservation (Decreto 1594, 1984). In Ciénaga de Mallorquín, DO behavior may be related to the features of external discharges entering the water body. In addition, water circulation and flux interchange, caused by winds and tide penetration, cause a permanent re-aeration of water within the lagoon.

Nitrate and phosphate concentrations

NO_3 concentrations averaged 3.28 mg/L during the transition period, with a minimum of 1.76 mg/L and a maximum of 5.09 mg/L (Fig. 8). During the simulation days, NO_3 concentrations varied, with low values during the first day, intermediate levels in days 2 to 4, and high concentrations during the sixth day of simulation. During the sixth day, the highest concentrations were observed in the area adjacent to the coast, as well as in the west and east zones. For the wet season, nitrate concentration average was 3.14 mg/L, with minimum and maximum levels of 1.98 mg/L and 3.34 mg/L, respectively (Fig. 8). NO_3 concentrations were higher during the transition period. The same spatial pattern found during the transition period was observed in the sixth day of simulation, with minimum concentrations in the

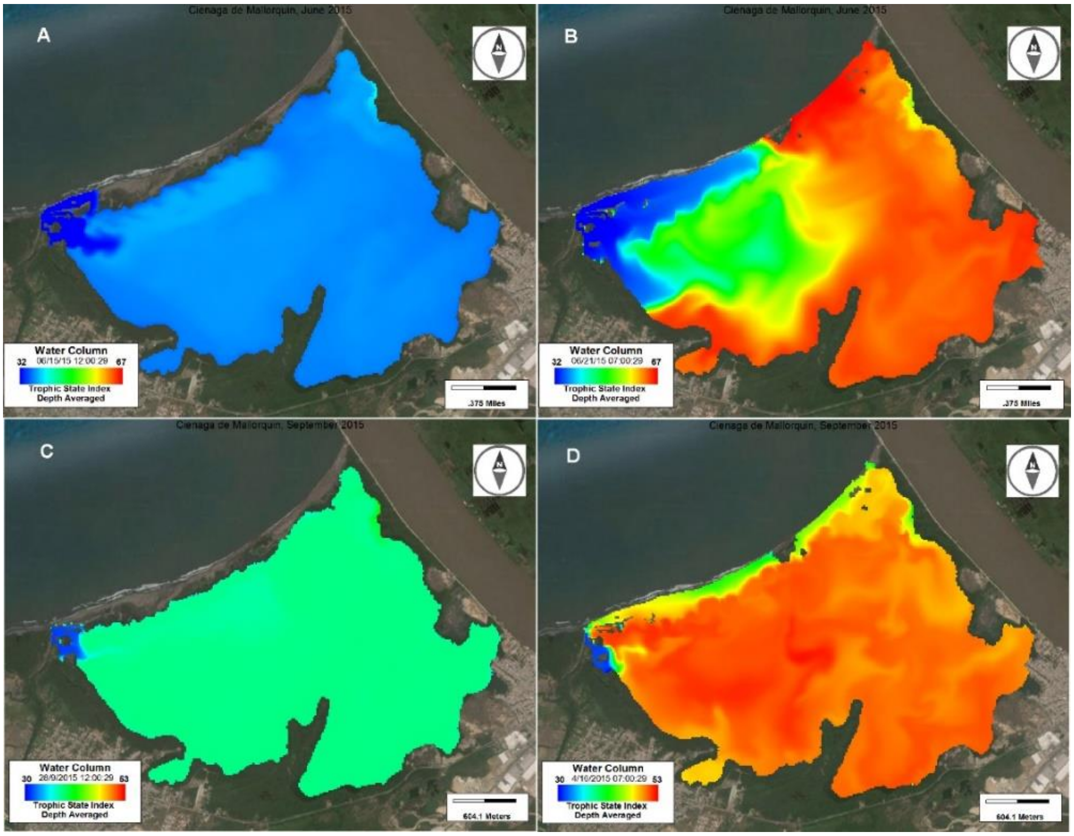

Fig. 10: Simulation of TSI variation. A) Transition Period (0.5 days of simulation). B) Transition Period (6 days of simulation). C) Wet season (0.5 days of simulation). D) Wet season (6 days of simulation) (wet season: note the change in scale values).

first simulation day and maximum values in the sixth day of simulation. In the same way, during both the analyzed periods, the lowest concentrations were found in the area influenced by the connection with the Caribbean Sea.

Average PO_4 concentration in Ciénaga de Mallorquín was 0.30 mg/L during the transition period, with a minimum of 0.24 mg/L and a maximum of 0.64 mg/L (Fig. 9). During the 6 days of simulation, intermediate PO_4 values were associated to the area influenced by the Arroyo León stream mouth. The highest PO_4 concentrations (>0.30 mg/L) were found for the three first days of simulation and reduced towards intermediate concentrations (0.26 mg/L) in the sixth day of simulation. For PO_4 obtained in the wet season, the average value as 0.20 mg/L, with a minimum of 0.19 mg/L and a maximum of 0.36 mg/L (Fig. 9). Overall, concentrations in the wet season were lower than in the transition period. However, the same pattern was observed at the entrance of Arroyo León, where intermediate concentrations (0.26 mg/L) were obtained. On the other side, in the east margin high PO_4 concentrations (0.30 mg/L) were observed in the zone where box culverts communicate the lagoon with the Magdalena River.

Nutrients are transported into coastal water bodies by surface water and groundwater fluxes, as well as by water interchange with the ocean (Anthony *et al.,* 2009). Primary production in coastal lagoons is regulated by the amount and variation of N and P (Romero-Sierra *et al.,* 2018). Surface NO_3 concentrations found in this study were above those of PO_4, in a 15-16:1 ratio, keeping up with Redfield ratios, which is a good indication of the relationship between Nitrogen and Phosphorus cycles (Babbin *et al.,* 2014). Nutrient concentrations in Ciénaga de Mallorquín may indicate the influx of waters rich in N and P. In addition, internal nitrification and denitrification processes do not show significant alterations within the evaluated time periods (Conan *et al.,* 2017). Likewise, obtained NO_3 and PO_4 concentrations are below the limits established by Colombian laws (Decreto 1594, 1984). Nevertheless, nutrient concentrations were high compared to other similar ecosystems (Conan *et al.,* 2017; Rodellas *et al.,* 2018). During the transition period nutrient concentrations were higher. Variation between both study periods may be related to water replacement processes in the lagoon. The highest concentrations of NO_3 occurred close to the coast, suggesting that the input of N might be caused by influx of coastal waters into the lagoon (Conan *et al.,* 2017). The main PO_4 contribution is associated to Arroyo León stream. Wastewaters from the city of Barranquilla, spilled into the stream, are characterized by a high organic load.

Trophic State Index

For the transition period, the average of calculated TSI values was 58.28, with a minimum of 31.32 and a maximum of 66.82. The average value represents a eutrophic state (Fig. 10). In the simulation period, the first day displayed the lowest TSI values (mesotrophic), increasing towards the sixth simulation day, when it reaches the highest values. In all cases, the zone closest to Arroyo León and to the connection to the sea displayed the lowest values of this index. The similar patterns were observed during the simulation days in the wet season (Fig. 10). Likewise, the lowest index values were observed at the entrance of Arroyo León.

Nutrient dynamics allows to understand trophic state, as nutrients may limit or promote primary production (Romero-Sierra *et al.,* 2018). The use of trophic state is useful for the management of water body eutrophication and productivity, making it particularly important in aquatic ecosystems (Carlson, 1977). Eutrophication is characterized by excessive phytoplankton blooming that causes hypoxia and reduced light penetration (Glibert *et al.,* 2010), which in turn results in trophic chain changes and biodiversity loss (NRC, 2000). The results of this research indicated that Ciénaga de Mallorquín behaved as mesotrophic and eutrophic during both study periods (transition period and wet season). In other words, Ciénaga de Mallorquín high productivity levels with temporal variations (Decreto 1594, 1984). During the transition period, the lagoon-ocean connection was close to the mouth of Arroyo León stream, contributing to nutrient increasing in this area. Arroyo León has significant concentrations of these parameters due to the wastewater spills the stream receives on its course to the lagoon.

CONCLUSION

Modelling and simulation of coastal ecosystems is of great environmental interest and scientific value, since it has been established as an efficient tool for the development of policies for endangered ecosystem protection. The EFDC Explorer model used for this research was well adjusted to the observed conditions in Cienaga de Mallorquín. Therefore, it was a reliable tool to evaluate changes in hydrodynamics and concentration distributions water quality variables during transition period and wet season. It was found that average velocities were between 0.006 m/s for the transition period and 0.013 m/s for the wet season. The temperature was above 29 degrees in both periods. DO concentrations were around 6.6 mg/L in both periods. Regarding the nutrient concentrations, NO_3 concentrations average were 3.28 mg/L and 3.14 mg/L in transition period and wet season. While, PO_4 concentrations average varied between 0.30 mg/L and 0.20 mg/L. The TSI calculation showed values close to 60 in both seasons, revealing areas of poor quality: from eutrophic to almost hypertrophic state. It was shown that the main contribution to eutrophication in the Ciénaga is given by the discharges of the Arroyo León. Vulnerable areas are close to the mixing zone of the Arroyo León, which, together with the pollutant load from the Magdalena River, are the factors that have mainly increased the problem of contamination in the lagoon, causing an imbalance in its sustainability. Therefore, local environmental authorities must take control measures to reduce nutrient levels from the water flows that feed Ciénaga de Mallorquín. In agreement with water quality criteria and Colombian normativity, parameter assessment averages indicate that in most cases Ciénaga de Mallorquín fulfills the standards stablished by current Colombian law. However, discharges and spills control measures must be implemented, given the declaration of Ciénaga de Mallorquín as a Ramsar site of international ecological and social importance. In addition, future studies must be implemented, including more water quality parameters and more extensive monitoring, in order to encompass different climatic seasons and environmental conditions in the study zone.

AUTHOR CONTRIBUTIONS

F. Torres-Bejarano performed the experimental design, implemented numerical model and prepared the manuscript text. A.C. Torregroza-Espinosa compiled the data and manuscript preparation. E. Martínez-Mera helped in the literature review and manuscript preparation. D. Castañeda-Valbuena helped in the literature review and manuscript preparation. M.P. Tejera performed the sampling campaigns and experiments.

ACKNOWLEDGEMENT

The authors acknowledge the collaboration of fishermen's association of Ciénaga de Mallorquin for their support during measurement and sampling campaigns.

CONFLICT OF INTEREST

The author declares that there is no conflict of interests regarding the publication of this manuscript. In addition, the ethical issues, including plagiarism, informed consent, misconduct, data fabrication and/or falsification, double publication and/or submission, and redundancy have been completely observed by the authors.

ABBREVIATIONS

°C	Degree Celsius
Ab	vertical turbulent diffusivity
ADCP	Acoustic Doppler Current Profiler
AH	Horizontal turbulent eddy diffusivity
Av	vertical turbulent eddy viscosity
C	Concentration or intensity of transport constituent
CE-QUAL-IC	Three-dimensional, time-variable, eutrophication model
CE-QUAL-W2	water quality and hydrodynamic model in 2D (longitudinal-vertical)
CIOH	Caribbean Oceanographic and Hydrographic Research Institute
COD	Dissolved oxygen concentration
CORMAGDALENA	Corporación Autónoma Regional del Río Grande de la Magdalena
CRA	Corporación Autónoma Regional del Atlántico
DO	Disolved oxygen
DOC	Dissolved organic carbon
DOs	saturated concentration of dissolved oxygen
EFDC	Environmental Fluid Dynamics Code
EPA	Environmental Protection Agency
f	Coriolis parameter
GPS	Global Positioning System
H	Total water depth
h	Hour
$H = h+\zeta$	Total depth, is the sum of depth and free surface
IDEAM	Institute of Hydrology, Meteorology and Environmental Studies
ITCZ	Intertropical Convergence Zone
L	Length (Units)
M	Mass (Units)
m/s	meters per second
m^3/s	Cubic meters per second
mg O2/L	miligrams of O2 per liter
mg/L	miligrams per liter
MINAMBIENTE	Ministerio del medio ambiente de Colombia
ML^{-2}/T	Mass X square length over time (Units)
ML^{-3}	Mass X cubic length (Units)
MT^{-1}	Mass X time (Units)
m_x, m_y	Square roots of the diagonal components of the metric tensor "m"
NH_4	Ammonium nitrogen concentration
NO_3	Nitrates
NRC	National Research Council
P	Physical pressure in excess of the reference density hydrostatic pressure
PO_4	Phosphates
PPT	Part per trillion
QS, QT	Horizontal diffusion and thermal sources and sinks
Qu, Qv	momentum source-sink terms

RAMSAR	Convención Ramsar
RMSE	Root Mean Square Error
S	water salinity
Sc	Source/sink term for the constituent
T	water temperature
TSI	Carlson's Trophic State Index
U, V	Horizontal velocity components in the curvilinear coordinates
UNEP	United Nations Environment Programme
Uninorte	Universidad Del Norte
W	Vertical velocity component
W_{sc}	Positive settling velocity when C represents a suspended material
X, Y	Orthogonal curvilinear coordinates in the horizontal direction
Z	Sigma coordinate
ΔX	Variation in elements in the X axis of numerical grid used for Ciénaga de Mallorquín
ΔY	Variation in elementss in the Y axis of numerical grid used for Ciénaga de Mallorquín
ρ	Water density

REFERENCES

Andrade, C.A., (2001). Las corrientes superficiales en la cuenca de Colombia observadas con boyas de deriva. Revista Acad. Colomb. Ci. Exact., 25(96): 321-335 **(15 pages).**

Anthony, A.; Atwood, J.; August, P.; Byron, C.; Cobb, S.; Foster, C.; Fry, C.; Gold, A.; Hagos, K.; Heffner, L.; Kellogg, D. Q.; Lellis-Dibble, K.; Opaluch, J.J.; Oviatt, C.; Pfeiffer-Herbert, A.; Rohr, N.; Smith, L.; Smythe, T.; Swift, J.; Vinhateiro, N., (2009). Coastal Lagoons and Climate Change: Ecological and Social Ramifications in US Atlantic and Gulf Coast Ecosystems. Ecol. Soc., 14(1): 8.

Arrieta, L.; Rosa, J., (2000). Distribución espacio-temporal de la mojarra rayada (*Eugerres plumieri*) en la ciénaga de Mallorquín. Tesis de grado, Univ. del Atlántico, Barranquilla **(78 pages)**.

Arrieta, L.; Rosa Muñoz, J., (2003). Estructura de la comunidad íctica de la Ciénaga de Mallorquín, Caribe colombiano. Bol. Investig. Mar. Costeras – Invemar., 32(1): 231-242 **(12 pages).**

Babbin, A.R.; Keil, R.G.; Devol, A.H.; Ward, B.B., (2014). Organic Matter Stoichiometry, Flux, and Oxygen Control Nitrogen Loss in the Ocean. Science., 34(6182): 406-408 **(3 pages).**

Carlson, R. E., (1977). A trophic state index for lakes. Limnol. Oceanogr., 22(2): 361-369 **(9 pages).**

Chapman, P.M., (2012). Management of coastal lagoons under climate change. Estuar. Coast. Shelf Sci., 110, 32-35 **(4 pages).**

Cioffi, F.; Di Eugenio, A.; Gallerano, F., (1995). A new representation of anoxic crises in hypertrophic lagoons. Appl. Math. Model., 19(11): 685-695 **(11 pages).**

Conan, P.; Pujo-Pay, M.; Agab, M.; Calva-Benítez, L.; Chifflet, S.; Douillet, P.; Dussud, C.; Fichez, R.; Grenz, C.; Gutierrez-Mendieta, F.; Origel-Moreno, M.; Rodríguez-Blanco, A.; Sauret, C.; Severin, T.; Tedetti, M.; Torres-Alvarado, R.; Ghiglione, J.F., (2017). Biogeochemical cycling and phyto-and bacterioplankton communities in a large and shallow tropical lagoon (Términos Lagoon, Mexico) under 2009–2010 El Niño Modoki drought conditions. Biogeosci., 14(4): 959-975 **(17 pages).**

Contreras, F.; Castañeda, O., (2004). La biodiversidad de las lagunas costeras. Ciencias., 76: 46-56 **(11 pages).**

Devkota. J.; Fang, X.; Fang, V., (2013). Response Characteristics of the Perdido and Wolf Bay System to Inflows and Sea Level Rise. Br. J. Environ. Clim. Change., 3(2): 229-256 **(28 pages)**.

Fertig, B.; Kennish, M.J.; Sakowicz, G.P., (2013). Changing eelgrass (Zostera marina L.) characteristics in a highly eutrophic temperate coastal lagoon. Aquat. Bot., 104: 70-79 **(10 pages).**

Galvis, O.S.; Téllez.; A. Lora., (1992). Contribución al conocimiento de las características medio-ambientales de la ciénaga de Mallorquín. VIII Seminario Nacional Ciencia Tecnol. Mar,1: 483-489 **(7 pages).**

Garcés-Ordóñez, O.; Vivas-Aguas, L.J.; Martínez, M.; Córdoba, T.; Contreras, A.; Obando, P.; Moreno, Y.; Muñoz, J.; Nieto, Y.; Ríos, M.; Sánchez, S.; Sánchez, D., (2016 a). Diagnóstico y Evaluación de la Calidad de las Aguas Marinas y Costeras del Caribe y Pacífico colombianos. Serie de Publicaciones Periódicas del Invemar No. 4. Red de vigilancia para la conservación y protección de las aguas marinas y costeras de Colombia (REDCAM). Informe técnico. INVEMAR, MADS y CAR costeras. Santa Marta **(347 pages).**

García-Oliva, M.; Pérez-Ruzafa, Á.; Umgiesser, G.; McKiver, W.; Ghezzo, M.; De Pascalis, F.; Marcos, C., (2018). Assessing the hydrodynamic response of the Mar Menor lagoon to dredging inlets interventions through numerical modelling. Water, 10(7): 959-992 **(33 pages).**

Glibert, P.M.; Burkholder, J.M., (2011). Harmful algal blooms and eutrophication: "strategies" for nutrient uptake and growth outside the Redfield comfort zone. Chin. J. Oceanol. Limnol., 29(4): 724-738 **(15 pages).**

Hamrick, J.M., (1992). A Three-Dimensional Environmental Fluid Dynamics Computer Code: Theoretical and computational aspects. Special report in applied marine science and ocean engineering, no. 317. Virginia Institute of Marine Science, College of William and Mary **(65 pages).**

Harley, C.D.G.; Hughes, A.R.; Hultgren, K.M.; Miner, B.G.; Sorte, C.J.B.; Thornber, C.S.; Rodriquez, L.F.; Tomanek., L.; Williams. S.L., (2006). The impacts of climate change in coastal marine systems. Ecol. Lett., 9(2): 228-241 **(14 pages).**

Hull, V.; Mocenni, C.; Falcucci, M.; Marchettini, N., (2000). A trophodynamic model for the lagoon of Fogliano (Italy) with ecological dependent modifying parameters. Ecol. Model., 134: 153–167 **(15 pages).**

Hur, J.; Lee, B.M.; Lee, T.H.; Park, D.H., (2010). Estimation of biological oxygen demand and chemical oxygen demand for combined sewer systems using synchronous fluorescence spectra. Sensors. 10(4): 2460-2471 **(12 pages).**

Itoh, S.; Takeshige, A.; Kasai, A., (2018). Modeling the coastal ecosystem complex: present situation and challenges. Fish Sci., 84: 293–307 **(14 pages).**

Jeong, S.; Yeon, K.; Hur, Y.; Oh, K., (2010). Salinity intrusion characteristics analysis using EFDC model in the downstream of Geum River. J. of Environ. Sci., 22 (6), pp 934-939 **(6 pages)**.

Ji, Zhen-Gang., (2017). Hydrodynamics and Water Quality: Modeling Rivers, Lakes, and Estuaries. Ed. John Wiley & Sons Inc., second edition **(581 pages)**.

Jiang, J.; Ri, T.; Pang, T.; Wang, Y.; Wang, P., (2019). Water quality management of heavily contaminated urban rivers using water quality analysis simulation program. Global J. Environ. Sci. Manage., 5(3): 295-308 **(13 pages)**.

Jiménez, P.A.L.; Alemany, V.E.; Alberola, M.C.; Solano, F.J.M., (2003). Metodología para la calibración de modelos de calidad de aguas. Ingeniería del agua., 10(4): 501-516 **(16 pages).**

Jones, N.R.; McMahon, A.T.; Bowler, M.J., (2001). Modelling historical lake levels and recent climate change at three closed lakes, Western Victoria, Australia (c.1840–1990). J. Hydrol., 246(1–4): 159–180 **(22 pages).**

Joos, F.; Plattner, G.K.; Stocker, T.F., Körtzinger., A.; Wallace, D.W.R., (2003). Trends in marine dissolved oxygen: implications for ocean circulation changes and the carbon budget. Eos, Transactions, American Geophysical Union, 84(21): 197-207 **(8 pages).**

Kennish, M.J.; Paerl, H.W., (2010). Coastal lagoons: critical habitats of environmental change. CRC Press, First ed. New York, NY **(555 pages).**

Liu, H.; Zheng, Z.C.; Young, B.; Harris, T.D., (2019). Three-dimensional numerical modeling of the cyanobacterium Microcystis transport and its population dynamics in a large freshwater reservoir. Ecol. Model., 398; 20-34 **(15 pages).**

Luo, F.; Li, R., (2009). 3D Water environment simulation for North Jiangsu offshore sea based on EFDC. JWARP. Prot., 1(1): 41-47 **(7 pages).**

Luo, X.; Li, X., (2018). Using the EFDC model to evaluate the risks of eutrophication in an urban constructed pond from different water supply strategies. Ecol. Model., 372: 1-11 **(11 pages).**

Marreto, R.N.; Baumgarten, M.G.Z.; Wallner-Kersanach, M., (2017). Trophic quality of waters in the Patos Lagoon estuary: a comparison between its margins and the port channel located in Rio Grande, RS, Brazil. Ac. Limn. Brasil., 29: 1-11 **(11 pages)**.

McCuen, R.H.; Knight, Z.; Cutter, A.G., (2006). Evaluation of the Nash–Sutcliffe efficiency index. J. Hydrol. Eng., 11(6): 597-602 **(6 pages).**

Ministerio de Ambiente y Desarrollo Sostenible. 1984. Decreto 1594. Usos del agua y residuos líquidos **(52 pages).**

Miranda, L.B.; Castro, B.M.; Kjerfve, B., (2002). Princípios de oceanografia física de estuários. São Paulo: Ed. da Universidade de São Paulo **(417 pages).**

National Research Council., 2000. Clean coastal waters: understanding and reducing the effects of nutrient pollution. National Academy Press **(428 pages).**

Newton, A.; Icely, J.; Cristina, S.; Brito, A.; Cardoso, A.C.; Colijn, F.; Zaldívar, J.M., (2014). An overview of ecological status, vulnerability and future perspectives of European large shallow, semi-enclosed coastal systems, lagoons and transitional waters. Estuarine Coast. Shelf Sci., 140: 95–122 **(28 pages).**

Newton, A.; Brito, A.C.; Icely, J.D.; Delorez, V.; Clara, I.; Angus, S., (2018). Assessing, quantifying and valuing the ecosystem services of coastal lagoons. J. Nat. Conserv., 44, 50–65 **(15 pages)**.

Panda, U.S.; Mahanty, M.M.; Rao, V.R.; Patra, S.; Mishra, P., (2015). Hydrodynamics and water quality in Chilika Lagoon-A modelling approach. Procedia Eng., 116: 639-646 **(8 pages).**

Park, K.; Jung, H.S.; Kim, H.S.; Ahn, S.M., (2005). Three-dimensional hydrodynamic eutrophication

model (HEM-3D): application to Kwang-Yang Bay, Korea. Mar. Environ. Res., 60: 171–193 (23 pages).

Parson, T.R.; Maitia, Y.; Lalli, C.M., (1984). A manual of Chemical and Biological Methods for Sea Water Analysis. Pergamonn Press, Oxford **(135 pages).**

Pérez-Ruzafa, A.; Marcos, C.; Pérez-Ruzafa, I.M.; Pérez-Marcos, M., (2011). Coastal lagoons: “transitional ecosystems” between transitional and coastal waters. J. Coast. Conserv., 15(3): 369-392 **(24 pages).**

Pérez-Ruzafa, A.; Marcos, C., (2012). Fisheries in coastal lagoons: An assumed but poorly researched aspect of the ecology and functioning of coastal lagoons. Estuarine Coastal Shelf Sci., 110:15–31 **(17 pages).**

Pérez-Ruzafa, A.; Pérez-Ruzafa, I. M.; Newton, A.; Marcos, C., (2019). Coastal lagoons: environmental variability, ecosystem complexity and goods and services uniformity, in Coasts and Estuaries, the Future, eds E. Wolanski, J. Day, M. Elliott, and R. Ramesh (New York, NY: Elsevier), 253–276 **(23 pages)**.

Poveda, G., (2004). La hidroclimatología de Colombia: una síntesis desde la escala inter-decadal hasta la escala diurna. Revista Acad. Colomb. Ci. Exact. 28(107): 201-222 **(22 pages).**

Quamrul, A.; Benson, B.; Visser, J.; Gang, D., (2016). Response of estuarine phytoplankton to nutrient and spatio temporal pattern of physico-chemical water quality parameters in little Vermilion Bay, Louisiana. Ecol. Inf., 32: 79-90 **(12 pages).**

Ramesh, R.; Chen, Z.; Cummins, V.; Day, J.; D’Elia, C.; Dennison, B.; Forbes, D.L.; Glaeser, B.; Glaser, M.; Glavovic, B.; Kremer, H.; Lange, M.; Larsen, J.N.; Le Tissier, M.; Newton, A.; Pelling, M.; Purvaja, R.; Wolanski, E., (2015). Land–ocean interactions in the coastal zone: Past, present and future. Anthropocene., 12: 85-98 **(13 pages).**

Rodellas, V.; Stieglitz, T.C.; Andrisoa, A.; Cook, P.G.; Raimbault, P.; Tamborski, J.J.; Beek, P.; Radakovitch, O., (2018). Groundwater-driven nutrient inputs to coastal lagoons: The relevance of lagoon water recirculation as a conveyor of dissolved nutrients. Sci. Total Environ., 642 (15): 764-780 **(17 pages).**

Romero-Sierra, P.; Rivas, D.; Almazán-Becerril, A.; Hernández-Terrones, L., (2018). Hydrochemistry and hydrodynamics of a Mexican Caribbean Lagoon: Nichupté Lagoon System. Estuar. Coast. Shelf Sci., 215: 185-198 **(14 pages).**

Shin, S.; Her, Y.; Song, J.H.; Kang, M.S., (2019). Integrated sediment transport process modeling by coupling Soil and Water Assessment Tool and Environmental Fluid Dynamics Code. Environ. Modell. Software. 116: 26-39 **(14 pages).**

Torres-Bejarano, F.; Coba, J.P.; Cuevas, C.R.; León, H.R.; Rodelo, R.C., (2016). La modelación hidrodinámica para la gestión hídrica del embalse del Guájaro, Colombia. Rev. Int. Metod. Numer., 32(3): 163-172 **(10 pages).**

Torres-Bejarano, F.; Couder-Castañeda, C.; Ramirez-León, H.; Hernández-Gómez, J.J.; Rodriguez-Cuevas, C.; Herrera-Diaz, I.E.; Barrios-Piña, H., (2019). Numerical modelling of heavy metal dynamics in a river-lagoon system. Math. Problems Eng., Article ID 8485031 **(24 pages)**.

Tetra Tech., (2007). The Environmental Fluid Dynamics Code Theory and Computation. Volume 1: Hydrodynamics and Mass

Transport. Tetra Tech, Inc. Fairfax **(60 pages)**.
UNESCO., (1981). Tenth report of the Joint Panel on Oceanographic Tables and Standards. UNESCO Tech. Pap. in Marine Science No. 36. UNESCO, Paris, **(25 pages)**.
Velasco, A.M.; Pérez-Ruzafa, A.; Martínez-Paz, J. M.; Marcos, C., (2018). Ecosystem services and main environmental risks in a coastal lagoon (Mar Menor, Murcia, SE Spain): the public perception. J. Nat. Conserv., 43, 180–189 **(19 pages)**.
Wang, C.; Shen, C.; Wang, P.F.; Qian, J.; Hou, J.; Liu, J.J., (2013). Modeling of sediment and heavy metal transport in Taihu Lake, China. J. Hydrodyn., 25(3): 379–387 **(9 pages).**
Woodward, F.I., (1987). Climate and plant distribution. Cambridge University Press, Cambridge, UK **(188 pages).**
Xia, M.; Craig, P. M.; Wallen, C. M.; Stoddard, A.; Poulsen, J. M.; Peng, M.; Schaeffer, B.; Liu, Z., (2011). Numerical Simulation of Salinity and Dissolved Oxygen at Perdido Bay and Adjacent Coastal Ocean. J. of Coastal Res., 27 (1): 73-86 **(14 pages)**.
Xia, M.; Jiang, L., (2015). Influence of wind and river discharge on the hypoxia in a shallow bay. Oc. Dynamics., 65: 665–678 **(13 pages)**.
Zhang, C. X.; You, X. Y., (2017). Application of EFDC model to grading the eutrophic state of reservoir: Case study in Tianjin Erwangzhuang Reservoir, China. Eng. Appl. Comput. Fluid Mech., 11(1): 111-126 **(15 pages)**.
Zou, R.; Li, Y.; Zhao, L.; Liu, Y., (2014). Exploring the Mechanism of Catastrophic Regime Shift in a Shallow Plateau Lake: A Three-Dimensional Water Quality Modeling Approach. Developments in Env. Model., 26: 411-435 **(25 pages)**.

AUTHOR (S) BIOSKETCHES

Torres-Bejarano, F.M., Ph.D., Professor, Departamento de Ingeniería Ambiental, Universidad de Córdoba, Carrera 6 No. 77- 305, Montería, Colombia. Email: *franklintorres@correo.unicordoba.edu.co*

Torregroza-Espinosa, A.C., Ph.D. Candidate, Full Time Professor, Departamento de Gestión Industrial, Agroindustrial y de Operaciones, Universidad de la Costa, Barranquilla, Colombia. Email: *atorregr4@cuc.edu.co*

Martínez-Mera, E., M.Sc., Doctoral Student, Unidad Académica de Agricultura, Universidad Autónoma de Nayarit, México.
Email: *eliana.martinez@upr.edu*

Castañeda-Valbuena, D., M.Sc., Doctoral Student, Instituto Tecnológico de Tuxtla Gutiérrez, Depto. Ingeniería Química y Bioquímica. Tuxtla Gutiérrez, Chiapas, México. Email: *dacasval@gmail.com*

Tejera-González, M.P., M.Sc., Part Time Professor, Departamento de Ingeniería Civil y Ambiental, Universidad de la Costa, Barranquilla, Colombia. Email: *mariapaulinatejera22@gmail.com*

HOW TO CITE THIS ARTICLE

Torres-Bejarano, F.M.; Torregroza-Espinosa, A.C.; Martínez-Mera, E.; Castañeda-Valbuena, D; Tejera-González, M.P., (2020). Hydrodynamics and water quality assessment of a coastal lagoon using environmental fluid dynamics code explorer modeling system. Global J. Environ. Sci. Manage., 6(3): 289-308.

DOI: 10.22034/gjesm.2020.03.02

url: https://www.gjesm.net/article_38654.html